ECE 445

SENIOR DESIGN LABORATORY

FINAL REPORT

Glove Controlled Mouse

Team #20

KHUSHI KALRA
(khushik3@illinois.edu)
VALLABH NADGIR
(vnadgir2@illinois.edu)
VIHAANSH MAJHITHIA
(vjm5@illinois.edu)

TA: Frey Zhao

December 10, 2025

Abstract

We built a wearable Bluetooth glove mouse that converts wrist orientation and pinch gestures into real-time cursor control. A BMI088 IMU estimates the gravity vector to define stable control axes, giving drift-free motion without integrating velocity. Hall-effect sensors provide reliable click and scroll gestures, while a DRV2605L driver delivers immediate haptic confirmation. An ESP32-S3 unifies sensing, processing, and HID transmission with low overhead. A custom two-PCB design integrates power, IMU, gesture sensing, and haptics into a compact, wearable system that enables intuitive, surface-independent pointing.

Contents

1 Introduction

1.1 Problem Statement

Then you go into a subsection. In your text you can cite things like this [1], and reference other section such as appendices like Appendix **??**.

Conventional mice and trackpads confine input to a flat desktop surface and force users into constrained wrist and arm postures, which limits expressive motion and leads to fatigue during long sessions and creative tasks. Stylus and pen-tablet systems offer finer control but depend on dedicated hardware, fixed workspaces, and wired or desk-bound setups that do not translate well to mobile use. Camera based gesture interfaces remove the surface but require line of sight, controlled lighting, and external cameras that are fragile in cluttered or variable environments.

There is a need for a pointing device that is wearable, portable, and independent of external infrastructure while providing precise, intuitive control comparable to a traditional mouse. The core problem is to design a glove based input system that interprets free space wrist motion and discrete finger gestures as stable cursor movements and mouse actions, preserving user comfort and reliability during extended everyday use.

1.2 Solution

Our solution is a wearable glove mouse that replaces the traditional desk surface with free space wrist motion and pinch gestures. An ESP32-S3 module on the main PCB collects inertial data from a BMI088 accelerometer and gyroscope, estimates the gravity vector at startup, and defines orthogonal “right” and “up” axes on the glove frame. At runtime the firmware processes and maps IMU data to generate stable cursor motion over Bluetooth HID, independent of any physical surface.

Discrete actions are handled by a gesture subsystem built from four Hall effect sensors on a secondary PCB and small magnets on the thumb. Each pinch maps to left click, right click, or scroll events, with simple edge based logic and debouncing for robust detection. A DRV2605L haptic driver and ERM coin motor provide immediate tactile feedback for confirmed gestures and calibration events, so the user can operate without constantly looking at the screen. A single LiPo battery, AP2112K 3.3 V regulator, and compact two board layout integrate power, sensing, processing, wireless link, and haptics into a comfortable glove that delivers intuitive, portable, surface independent pointing.

1.3 High-Level Requirements

1. The system must produce a visible cursor update or haptic response less than 100 ms after a hand motion or finger gesture input.
2. The motion tracking subsystem must update the wrist orientation and cursor command signals at a rate of at least 100 Hz.
3. The gesture detection subsystem must recognize intentional click and scroll gestures with at least 97% accuracy while maintaining a false positive rate below 2%.

2 Design

2.1 Physical Design

The hardware is split across two PCBs to keep the glove light while preserving routing area and battery capacity. A main controller PCB rests on the forearm and carries the ESP32-S3 [2] module, power regulation, LiPo battery connector, and a 20 pin board to cable connector that fans out digital interfaces and power to the glove. This board concentrates the heavier components near the forearm, which reduces inertia on the hand and improves comfort during extended use.

A smaller secondary PCB mounts on the back of the hand and contains the BMI088 IMU, the DRV2605L haptic driver and ERM coin motor, and the headers that fan out to the Hall effect sensors at the fingertips. The IMU is placed near the wrist so its measured acceleration tracks bulk wrist orientation rather than local finger motion, while the haptic motor is located where vibrations are clearly felt without interfering with grasping. We house both the PCBs in 3D printed enclosures are shown in Figure 1

Four Hall effect switches are fixed near the pads of the index, middle, ring, and little fingers, with a small magnet attached to the thumb. Bringing the thumb close to a given fingertip pulls that sensor low and is interpreted as a specific gesture such as left click, right click, scroll up, or scroll down. Wiring from the fingertip sensors and thumb magnet returns along the back of the fingers to the hand PCB, then through the 20 conductor cable to the forearm board, with slack and strain relief chosen so that full wrist and finger motion does not stress the interconnects.

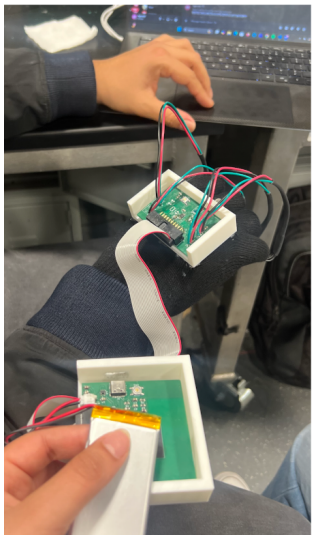

Figure 1: Physical layout of the system showing the main controller PCB mounted on the forearm, the sensor and haptic PCB on the back of the hand, and Hall effect sensors and wiring routed to the fingertips with a thumb mounted magnet for pinch gestures.

2.2 High-Level Block Diagram

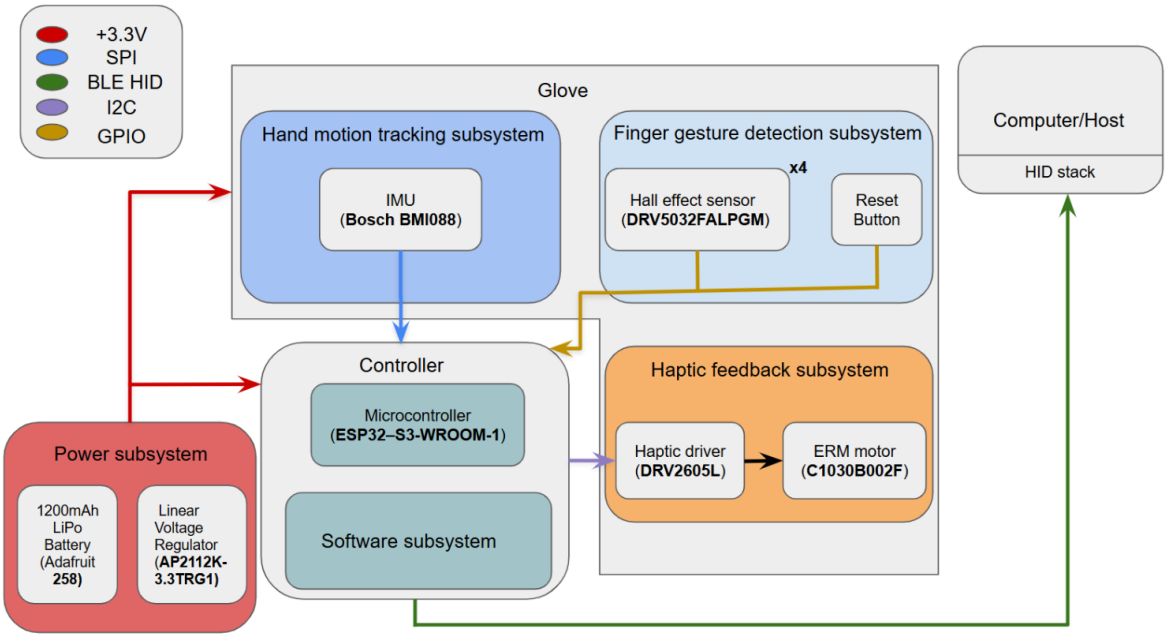

Figure 2: High-level block diagram showing major subsystems: hand-motion tracking, haptic feedback, finger gesture detection, software/controller, and the power subsystems.

2.3 Functional Overview and Subsystems

2.3.1 Hand Motion Tracking Subsystem

Overview

The hand-mounted tracking subsystem measures wrist orientation and dynamic acceleration using the BMI088 IMU [3]. The sensor is placed on the back of the hand near the wrist so that its readings capture global wrist motion rather than finger flexion. This subsystem provides the calibrated physical measurements required for cursor motion computation.

Sensor Configuration and Sampling

The BMI088 accelerometer operates at a sampling rate of approximately 1000 Hz, providing linear acceleration data along the device's three orthogonal axes. The IMU communicates with the ESP32-S3 over SPI routed through the 20-pin interconnect between the hand board and the forearm controller board. Proper routing length, ground-reference continuity, and decoupling capacitors were used to minimize noise and bus errors.

Electrical and Physical Integration The glove PCB contains the BMI088, haptic driver, and ERM motor, while the forearm-mounted PCB contains the ESP32-S3, power regulation, and battery interface. All IMU signals are routed to the controller board through a

20-pin cable. Pin-level wiring, routing, and decoupling details follow the Bosch reference design as shown in Figure 3.

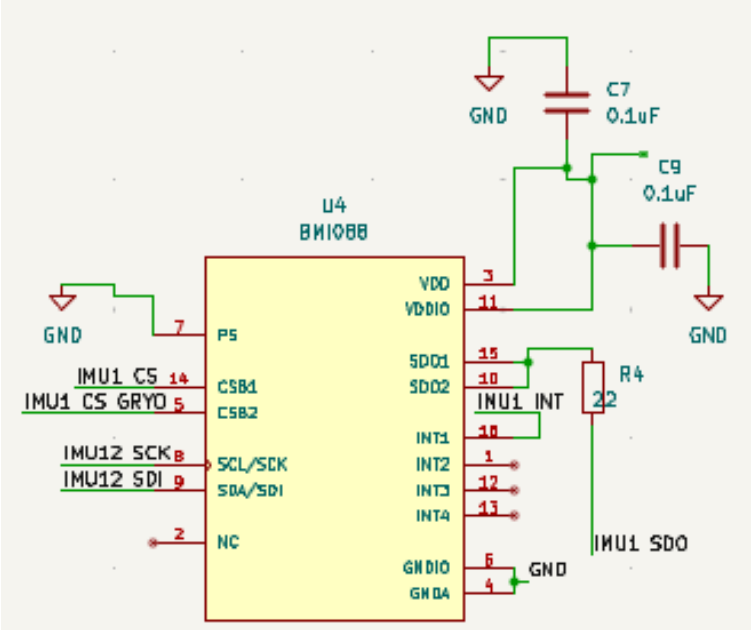

Figure 3: BMI088 accelerometer used for wrist motion tracking.

Gravity Vector Estimation

During startup, the subsystem collects 500 consecutive acceleration samples and computes their average to estimate the gravity vector in the IMU reference frame. This calibration step is necessary because small biases in the accelerometer and slight mounting misalignments produce incorrect orientation estimates if gravity is not explicitly modeled.

Linear Acceleration Extraction

At runtime, each accelerometer sample has the calibrated gravity vector subtracted to yield a linear acceleration signal corresponding to intentional wrist movement. A small deadzone is applied to suppress sensor noise when the hand is stationary. This produces a stable and drift-free motion signal, eliminating the need for velocity or position integration.

2.3.2 Software Subsystem

Overview

The software subsystem converts calibrated IMU measurements into reliable cursor motion commands. It computes a persistent orientation reference, performs filtering and projection operations, maps movements into screen-space deltas, and packages the output into BLE HID mouse events [4]. It also manages gesture-triggered haptic feedback and reset operations.

Coordinate Frame Construction

To produce repeatable cursor motion irrespective of wrist tilt, the software constructs a stable control frame from the IMU's gravity estimate and a nominal reference orientation. First, gravity is estimated by averaging a large batch of accelerometer samples with the hand held still. This yields a calibrated gravity vector g in the sensor frame.

The algorithm then selects a nominal candidate for the "right" direction based on which coordinate of g has the largest magnitude. Six canonical cases are used (gravity aligned with ±X, ±Y, or ±Z), and for each case a corresponding reference right and desired up direction is chosen. The reference right vector is projected onto the plane orthogonal to g, removing any component along gravity. This projection is normalized to form the canonical "right" direction, $\mathbf{e}_{\text{Right}}$, which lies in the plane perpendicular to gravity.

The "up" direction, $\mathbf{e}_{\text{Up}}$, is then computed as the normalized cross product

$$\mathbf{e}_{\text{Up}} = \frac{\mathbf{g} \times \mathbf{e}_{\text{Right}}}{\|\mathbf{g} \times \mathbf{e}_{\text{Right}}\|},$$

ensuring orthogonality between the control axes. If necessary, $\mathbf{e}_{\text{Up}}$ is flipped to align with a desired up direction from the canonical case. The resulting frame, $\{\mathbf{e}_{\text{Right}}, \mathbf{e}_{\text{Up}}\}$, provides stable axes for motion mapping that remain fixed until a reset is requested by the user.

Filtering and Deadzone Application

Each IMU reading is processed through a light smoothing filter to reduce high-frequency noise. A magnitude-based deadzone suppresses micro-motions and vibrations, ensuring that cursor drift does not occur when the hand is at rest.

Projection and Motion Mapping After gravity calibration and construction of the control frame, each new accelerometer sample is first corrected by subtracting the gravity reference. A small deadzone suppresses noise and unintentional micro-motions. The gravity-free acceleration vector is then normalized by g and projected onto the canonical control axes:

$$\text{rightNormRaw} = \mathbf{a}_{\text{lin}} \cdot \mathbf{e}_{\text{Right}}, \quad \text{upNormRaw} = \mathbf{a}_{\text{lin}} \cdot \mathbf{e}_{\text{Up}}.$$

These raw projections are smoothed using exponential filtering to reduce jitter while preserving responsiveness. The filtered normalized values are scaled into integer mouse

deltas (dx, dy), mapped via a configurable maximum cursor step per update. The final BLE HID mouse events are then sent to the host at roughly 100 Hz, yielding responsive cursor control with minimal drift. This process in illustrated in Figure 4

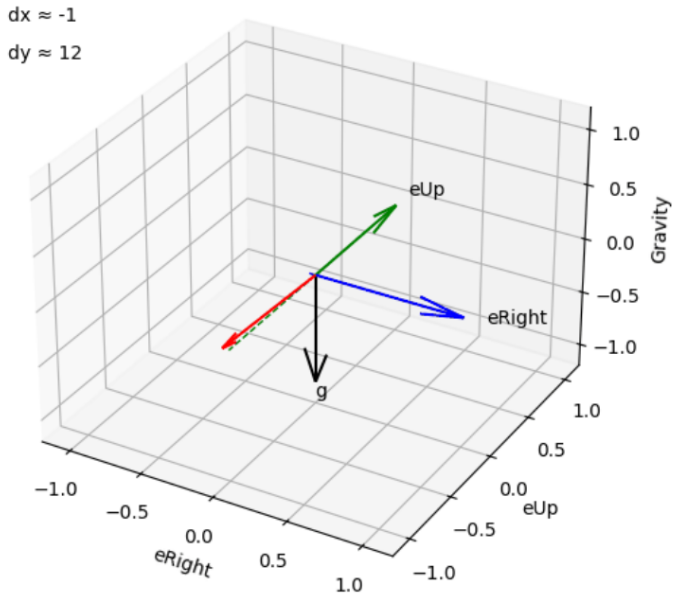

Figure 4: Red vector indicates the normalized accelration vector in the IMU's frame of reference.

Reset Mechanism

The reset button triggers immediate recomputation of the gravity vector and control axes. This allows the user to re-center their wrist orientation in any comfortable pose, enabling natural use across different hand positions without degrading control quality.

BLE HID Transmission

The ESP32-S3 formats the cursor deltas and gesture events into standard Bluetooth HID packets. These packets are transmitted at high rate to the host computer, providing responsive cursor motion and low perceived latency.

2.3.3 Finger Gesture Detection Subsystem

Overview

Finger gestures are detected using four Hall effect sensors mounted near the index, middle, ring, and little fingertips, with a small neodymium magnet attached to the thumb. Bringing the thumb near a sensor produces a distinct active-low signal that corresponds to a specific action: the index finger triggers left click, the middle finger triggers right click, the ring finger triggers scroll up, and the little finger triggers scroll down.

Electrical and Physical Integration

Each Hall sensor (DRV5032) [5]. is mounted at a fingertip and connected to the glove PCB, which routes all signals through the 20-pin cable to the ESP32-S3 on the forearm controller board. The sensors use internal pull-ups on the microcontroller and operate in active-low mode. Their placement ensures reliable activation while allowing natural finger movement.

Gesture Detection Logic

Click gestures (index and middle fingers) use a debounced falling-edge trigger to prevent false activations and guarantee one click per thumb–finger contact. Scroll gestures (ring and little fingers) use direct level detection without debounce, allowing smooth continuous scrolling when the thumb is held near the sensor. For each confirmed gesture, the ESP32-S3 issues the corresponding BLE HID mouse command and triggers a brief haptic pulse to provide immediate tactile feedback.

2.3.4 Haptic Feedback Subsystem

Overview

The haptic subsystem provides immediate tactile confirmation for user actions, ensuring that clicks, scrolls, and orientation resets feel responsive without requiring visual attention. This feedback reinforces gesture reliability and improves overall usability during free-space interaction.

Electrical and Physical Integration

The glove PCB includes a DRV2605L haptic driver [6] and a compact ERM coin motor. The DRV2605L communicates with the ESP32-S3 over I²C, routed through the same 20-pin interconnect used for the IMU and Hall sensors. The ERM motor is mounted on the back of the hand where vibrations are clearly perceptible but do not interfere with finger movement. Detailed wiring and register configurations are documented in Appendix X.

Feedback Logic

The haptic subsystem is triggered whenever a validated gesture or system event occurs. For click and scroll gestures, the controller plays a short waveform from the DRV2605L's internal library to acknowledge the action. A stronger effect is used during orientation recalibration to signal that a new neutral pose has been recorded. All haptic patterns run autonomously on the DRV2605L, allowing the ESP32-S3 to continue processing motion and gestures without blocking.

2.3.5 Power Subsystem

The power subsystem provides stable and sufficient electrical power to all components of the wearable glove mouse, including the ESP32-S3 microcontroller, BMI088 IMU, DRV2605L haptic driver, and the eccentric rotating mass (ERM) vibration motor. The system is powered by a single-cell 3.7 V lithium-polymer (LiPo) battery [7], chosen for its high energy density, low weight, and ability to source short-duration current spikes during wireless transmission and haptic activation.

Voltage Regulation

A LiPo cell ranges from 4.20 V when fully charged to approximately 3.0 V at depletion. Since all digital subsystems require a regulated 3.3 V supply, a low-dropout (LDO) voltage regulator (AP2112K-3.3 [8]) was selected. This regulator provides:

- 600 mA continuous output current,
- low dropout voltage (approx. 250 mV at 300 mA),
- low quiescent current ($\approx 55\ \mu$A),
- low output noise, beneficial for IMU stability.

These characteristics ensure that the power rail remains stable even during ESP32-S3 radio activity or ERM motor activation.

Current Consumption Analysis

Each subsystem was characterized to ensure the battery and regulator could safely support both average and peak-demand scenarios. Table 1 summarizes measured and datasheet-typical current draws.

Table 1: Typical Current Consumption of Major Subsystems

Subsystem	**Typical Current Draw**
ESP32-S3 (active + BLE HID)	22–30 mA
ESP32-S3 (transmit peak)	80–120 mA
BMI088 IMU	5.0–5.5 mA
Hall sensors (4 units)	< 0.01 mA total
DRV2605L haptic driver	1–2 mA
ERM vibration motor (typical)	55–60 mA
ERM vibration motor (worst-case)	80–100 mA

The highest-load condition occurs when the ESP32-S3 is transmitting BLE reports while the haptic subsystem is simultaneously driving the ERM motor. The measured peak cur-

rent during stress testing was approximately 110–130 mA, which is well within the safe operating region of the AP2112 regulator and the LiPo cell.

Battery Life Estimation

Average current during normal operation (IMU sampling, BLE reporting at 80–100 Hz, occasional haptic feedback) was measured at approximately 30–40 mA. Using the project's 1200 mAh LiPo battery, expected runtime is:

$$\text{Battery Life} = \frac{1200\ \text{mAh}}{35\ \text{mA}} \approx 34\ \text{hours}.$$

Under worst-case conditions, where the haptic motor is driven continuously (not representative of real use), expected runtime is:

$$\frac{1200\ \text{mAh}}{110\ \text{mA}} \approx 10.9\ \text{hours}.$$

Deep-sleep standby current of the ESP32-S3 (8–10 µA), plus regulator quiescent current (55 µA), results in an estimated theoretical standby life exceeding one year.

These results meet the project requirement of at least 2 hours of continuous functional runtime.

Power Distribution and Protection

To minimize noise coupling and voltage ripple, especially during ERM motor activation, the following design practices were implemented:

- Local decoupling capacitors placed near the IMU, ESP32-S3, and DRV2605L power pins.
- A star-ground topology separating high-current haptic return paths from sensitive IMU analog grounds.
- The DRV2605L's internal waveform shaping used to limit back-EMF from the ERM motor.
- A 500 mA resettable polyfuse added in series with the battery for overcurrent protection.
- The TP4056 charging module provides overcharge, over-discharge, and short-circuit protection for the LiPo cell.

Summary

The power subsystem reliably supports all components under typical and peak operation. The 1200 mAh LiPo battery, AP2112 LDO regulator, and protection circuitry ensure stable voltage delivery, long runtime, and user safety. Future improvements include integrating a dedicated fuel-gauge IC for real-time battery state-of-charge estimation and enabling deeper low-power firmware modes to further extend runtime.

2.4 Design Decisions

2.4.1 Shift from Velocity/Position Tracking to Gravity-Based Motion

Our original design proposed integrating linear acceleration to estimate wrist velocity and position over time. In practice, small accelerometer biases and noise caused rapid drift, even over a few seconds, leading to unusable cursor behavior (see Figure 5). Multi-IMU fusion and more complex filtering would have added significant algorithmic and computational complexity without guaranteeing robustness. We therefore adopted a gravity-referenced, projection-based method that treats changes in acceleration relative to a calibrated neutral pose as the control signal. This approach eliminates long-term drift, simplifies the software stack, and produces stable cursor motion across extended use.

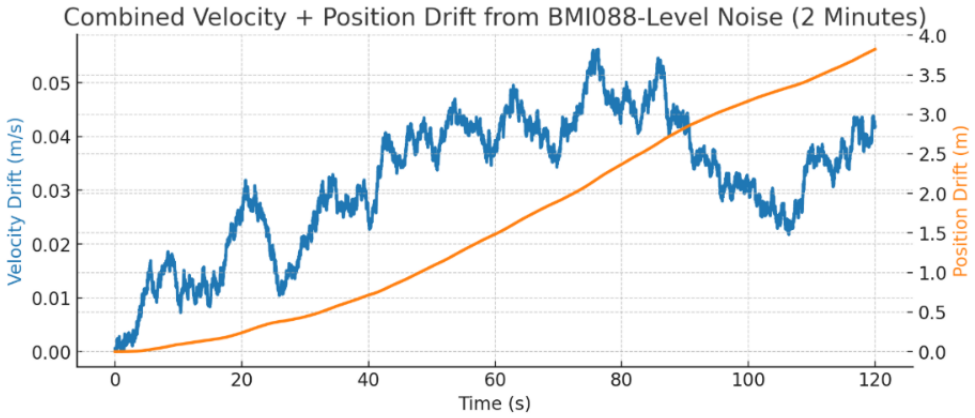

Figure 5: Growth of velocity/position drift assuming BMI088 noise levels.

2.4.2 Switch from ICM-20948 to BMI088 IMU

The original proposal specified an ICM-20948 nine axis IMU, chosen mainly from prior lab designs. Before ordering hardware, we revisited the sensor choice and compared datasheets, reference designs, and available software support. The BMI088 offered lower accelerometer noise, better bias and temperature stability, and a simpler integration path over SPI on the ESP32-S3, while still meeting our bandwidth and range requirements. Based on this analysis, we selected the BMI088 from the start of the build, avoiding additional fusion complexity and reducing risk to the motion tracking performance.

2.5 Hardware and PCB Design Choices

The electronics are implemented on PCBs: a controller board that sits on the forearm and a sensor/haptic board that mounts closer to the wrist and routes out to the finger sensors. This partitioning keeps the heavier components (ESP32-S3 module, USB-C connector, power LED, LDO) in a compact pod while allowing the IMU, DRV2605L haptic

driver, and Hall-effect sensor connectors to be placed where they best match the glove geometry.

A 2×10 board-to-board connector between the two PCBs carries 3.3V power, ground, SPI/I^2C buses, IMU interrupt lines, and four Hall sensor inputs. This approach gives a clean electrical break between the controller and sensing front-end and also makes debugging easier: either board can be replaced or reworked without disturbing the other.

The outline of the controller board is chosen so that it fits within the flat region on the back of the hand while leaving a large space for the ESP32-S3 antenna. The sensor board outline is wider and more rectangular so the IMU can sit near the physical wrist joint and the finger connectors can fan out symmetrically toward each finger.

Appendix A shows the final layout of the controller PCB. The ESP32-S3-WROOM-1 is centered on the board with its PCB antenna pointing into a dedicated keep-out zone. All supply pins of the module are surrounded by a solid ground pour on the top and bottom layers, stitched with vias.

The USB-C connector is placed along one edge of the controller PCB so that a cable can exit cleanly while coding. The D+ and D– traces from the ESP32-S3 USB pins to J1 are kept short, run in parallel, and have no sharp corners as using these layout practices reduce impedance discontinuities and improve signal integrity. The CC1 and CC2 pull-down resistors (R4 and R5) are routed directly to ground near the connector to clearly advertise a device role to the computer.

Routing on the controller board is predominantly on the top layer, with the bottom layer used as a near-continuous ground plane. Only a few short bottom-layer signal traces are used where necessary to escape dense pin fields. This provides a low-impedance return path for high-speed edges (USB, SPI clocks) and reduces EMI. The reset and boot buttons (SW2 and SW1) are placed on opposite sides of the module so they remain accessible even when the board is mounted inside the glove enclosure.

The second board carries the BMI088 IMU, the DRV2605L haptic driver, and four connectors for the Hall-effect sensors. The IMU is located close to the board center to better approximate wrist motion rather than finger motion.

The DRV2605L and its ERM motor connector are placed near one edge of the board so the motor wiring can exit cleanly toward the glove. The I^2C lines between the connector and the DRV2605L are routed as a tightly coupled pair with pull-ups placed near the driver. Acapacitor on the 3.3V rail provides extra current headroom during haptic pulses so that the IMU and hall sensors do not see appreciable supply droop.

Hall sensor connectors are arranged in a row along both sides of the board with identical pinouts (GND, 3.3 V, signal). This symmetry simplifies the harness and also allows any finger to be moved to any connector without changing the main board. Each connector's signal trace runs back to the board-to-board header. As with the controller board, both layers of the sensor PCB use large ground pours tied together by via stitching

These PCB and hardware design choices collectively ensure that the glove is compact and

comfortable while still meeting the electrical requirements for low-latency sensing, BLE communication, and stable power delivery.

3 Cost Analysis

3.1 Labor

Each team member contributed approximately 120 hours over the semester.

Team Member	Hours	Rate	Multiplier	Cost
Khushi Kalra	120	$40/hr	2.5	$12,000
Vallabh Nadgir	120	$40/hr	2.5	$12,000
Vihaansh Majithia	120	$40/hr	2.5	$12,000
Total Labor Cost				**$36,000**

Table 2: Labor cost estimate using the ECE 445 standard calculation.

3.2 Parts

Table 3 summarizes all components purchased for the project. Retail prices are provided for commercial viability analysis; department-provided components may be listed as $0 for accounting purposes. The table consolidates all items ordered through Digi-Key, Mouser, Amazon, and ECE 445 lab inventory.

3.3 Cost Summary

The overall cost of the project is summarized below:

- Total labor cost: $36,000
- Total parts cost: $142.76

Thus, the effective total cost of the prototype development is:

$$\boxed{\text{Total Project Cost} = \$36,142.76}$$

Part Description	Vendor	Qty	Unit Price	Ext. Price
BMI088 Accelerometer (16LGA)	Digi-Key	3	$4.71	$14.13
BMI088 Shuttle Board 3.0	Digi-Key	1	$14.40	$14.40
DRV2605L Haptic Driver Eval Board	Digi-Key	1	$7.95	$7.95
1.27 mm Conn Header (2-pos)	Digi-Key	3	$3.48	$10.44
DRV5032 Hall Sensors (10-pack)	Digi-Key	10	$0.26	$2.55
Li-Ion Battery 3.7 V 1.2 Ah	Digi-Key	1	$8.96	$8.96
NE1206 Magnets	Digi-Key	5	$0.41	$2.05
Header Sets (2–3 pos mixed)	Digi-Key	–	–	$5.00
ERM Vibration Motor 9 mm	Digi-Key	2	$2.99	$5.98
AP2112K-3.3 LDO Regulator	Digi-Key	2	$0.61	$1.22
DRV2605LDGST Motor Driver IC	Digi-Key	2	$3.02	$6.04
GPIO Ribbon Cable (2×10)	Digi-Key	1	$1.76	$1.76
IDC 20-pin Cable Assembly	Digi-Key	1	$9.01	$9.01
Conn Header R/A 20-pos (2.54 mm)	Digi-Key	4	$0.70	$2.80
USB-C PCB Receptacle	Amazon	2	$6.89	$13.78
Small Neodymium Magnets (Thumb)	Amazon	1	$5.99	$5.99
10×10 Header Blocks	Mouser	3	$3.87	$11.61
Total Parts Cost				**$142.76**

Table 3: Parts cost for the Glove Controlled Mouse prototype.

4 Conclusion

4.1 Accomplishments

We designed and built a fully integrated glove controlled mouse that performs real time cursor control, gesture based clicks and scrolling, and haptic feedback using a split PCB architecture on the glove and forearm. Quantitative testing showed that the system meets or exceeds the intended high level performance targets for end to end latency, motion update rate, and gesture reliability, while remaining comfortable enough for extended use. The final prototype demonstrates that free space, surface independent pointing can be achieved with a single IMU, simple Hall based gestures, and a BLE enabled microcontroller. :contentReference[oaicite:0]index=0

4.2 Challenges

The project required several rounds of hardware and firmware iteration. On the hardware side, the BMI088 footprint, fine pitch soldering, and SPI routing through the 20 pin harness demanded careful assembly and rework. On the firmware side, we experimented with velocity and position integration before converging on the gravity referenced projection method that removes drift and simplifies tuning. These challenges highlighted the importance of clean PCB layout, robust interconnects, and starting from a physically well conditioned signal path. :contentReference[oaicite:1]index=1

4.3 Ethical and Safety Considerations

From an ethical perspective, our primary responsibility is to ensure that the device operates safely and does not expose users to electrical, thermal, or long term ergonomic risks, consistent with the IEEE Code of Ethics **ieeeethics**. We limited operating voltages to 3.7–4.2 V on the battery side and 3.3 V on the logic side, provided adequate isolation and insulation between conductive traces and skin contact areas, and sized currents so that worst case haptic and radio loads stay well within component ratings. We also designed the glove to be removable, lightweight, and non restrictive so that it does not promote harmful wrist postures or repetitive strain beyond that of a conventional mouse. All reported performance metrics are based on actual measurements rather than idealized estimates, in line with the expectation to present results honestly and avoid misleading claims.

4.4 Future Work

Future work can extend the current design in several directions. On the hardware side, a flex PCB revision could replace jumper wires on the glove and improve robustness while reducing weight. On the software side, incorporating jerk based stopping logic and adaptive filtering could further reduce overshoot and improve fine control. Additional multi finger gestures, user specific calibration profiles, and battery state monitoring

would move the system closer to a product level device and broaden its applicability to creative and accessibility focused workflows. :contentReference[oaicite:3]index=3

References

[1] IEEE. ""IEEE Code of Ethics",” Accessed: Feb. 8, 2020. [Online]. Available: https://www.ieee.org/about/corporate/governance/p7-8.html.

[2] Espressif Systems, *ESP32-S3 Series: 2.4 GHz Wi-Fi and Bluetooth 5 (LE) SoC*, Datasheet and technical reference, 2022. [Online]. Available: https://www.espressif.com/en/products/socs/esp32-s3.

[3] B. Sensortec, *BMI088: Small, Versatile Inertial Measurement Unit*, Datasheet and product specification, 2018. [Online]. Available: https://www.bosch-sensortec.com/products/motion-sensors/imu/bmi088/.

[4] T-vK. “BleMouse Arduino Library.” Open-source BLE HID mouse library for ESP32. [Online]. Available: https://github.com/T-vK/ESP32-BLE-Mouse.

[5] Texas Instruments, *DRV5032: Ultra-Low-Power Digital Hall Effect Sensor*, Datasheet for fingertip Hall sensors, 2015. [Online]. Available: https://www.ti.com/product/DRV5032.

[6] Texas Instruments, *DRV2605L Haptic Driver for ERM/LRA*, Datasheet and application information, 2013. [Online]. Available: https://www.ti.com/product/DRV2605L.

[7] Adafruit. “1200 mAh 3.7 V LiPo Battery.” Product page for single-cell lithium polymer battery. [Online]. Available: https://www.adafruit.com/product/258.

[8] Diodes Incorporated, *AP2112K: 600 mA CMOS Low Dropout Regulator*, Datasheet for 3.3 V LDO regulator, 2014. [Online]. Available: https://www.diodes.com/part/view/AP2112K.

Appendix A PCB Designs

This appendix contains all PCB-related figures referenced in the report.

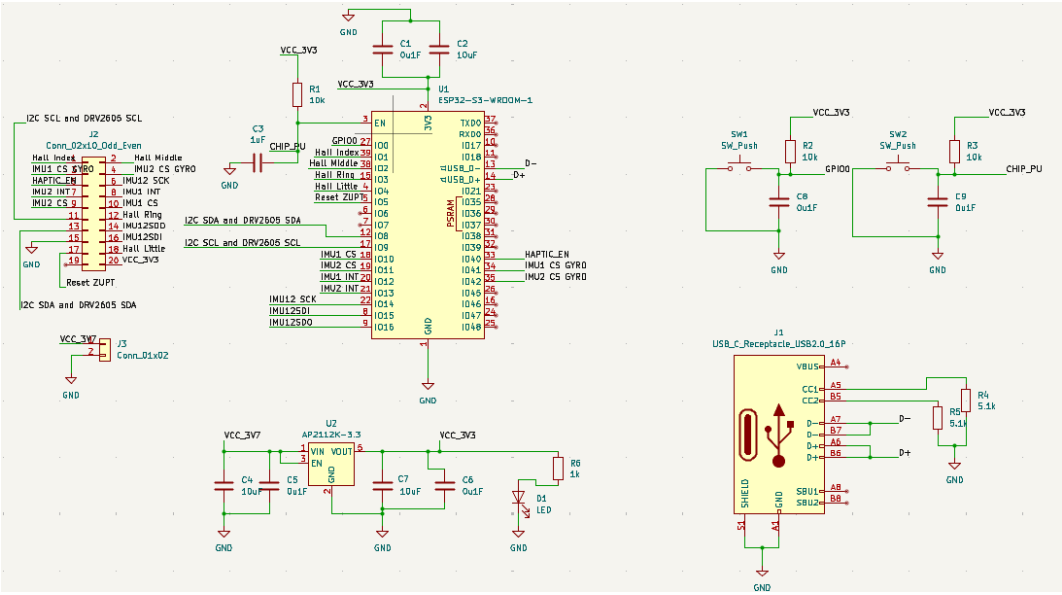

Figure 6: Rendered view of the forearm-mounted main PCB.

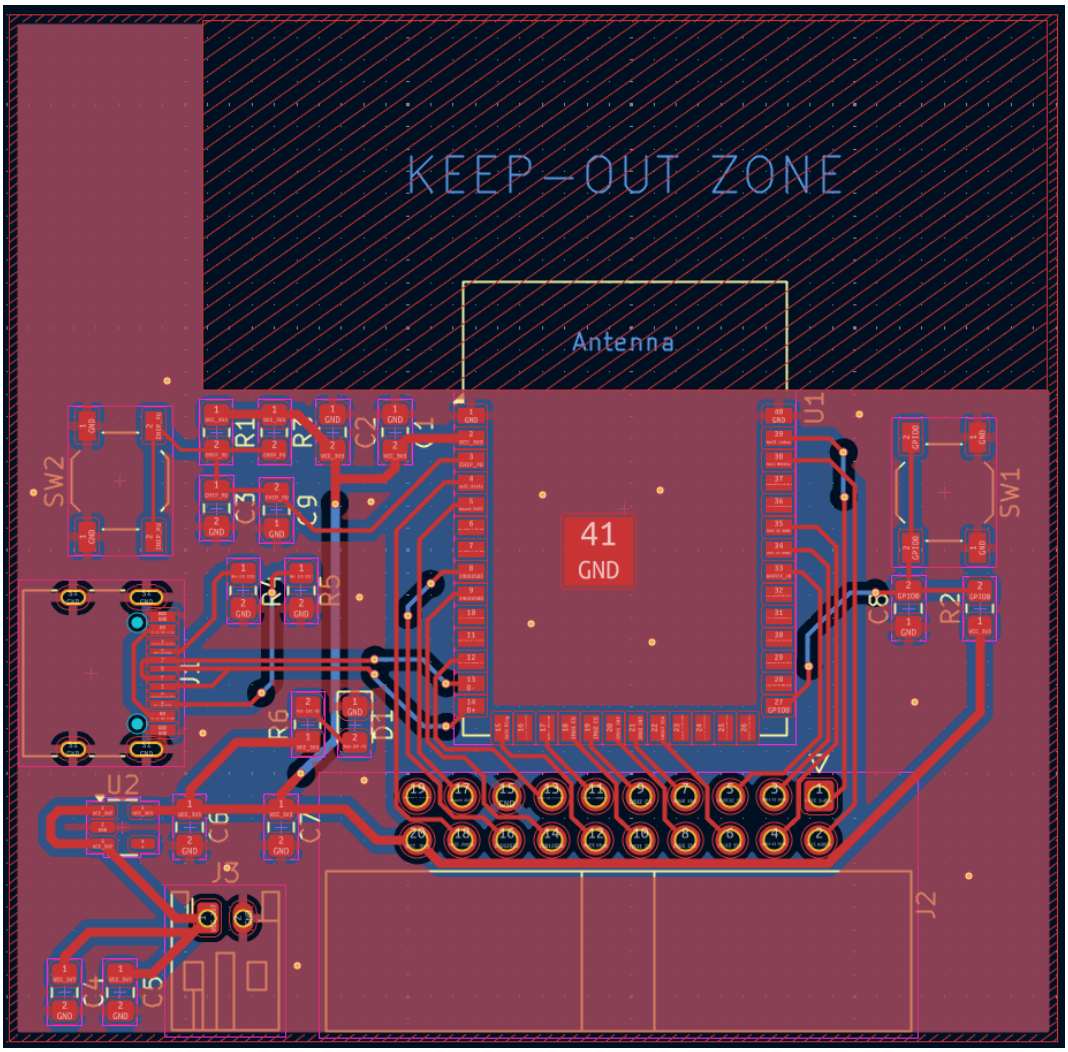

Figure 7: KiCad layout of the main controller PCB, showing routing and component placement.

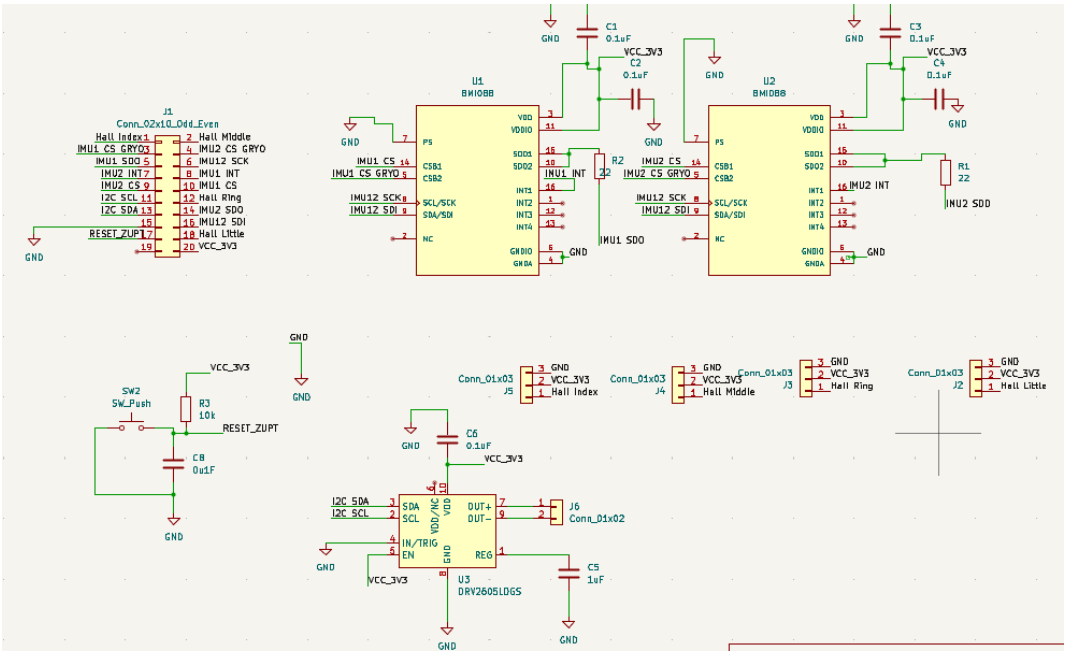

Figure 8: Rendered view of the glove-mounted secondary PCB containing IMU and haptics.

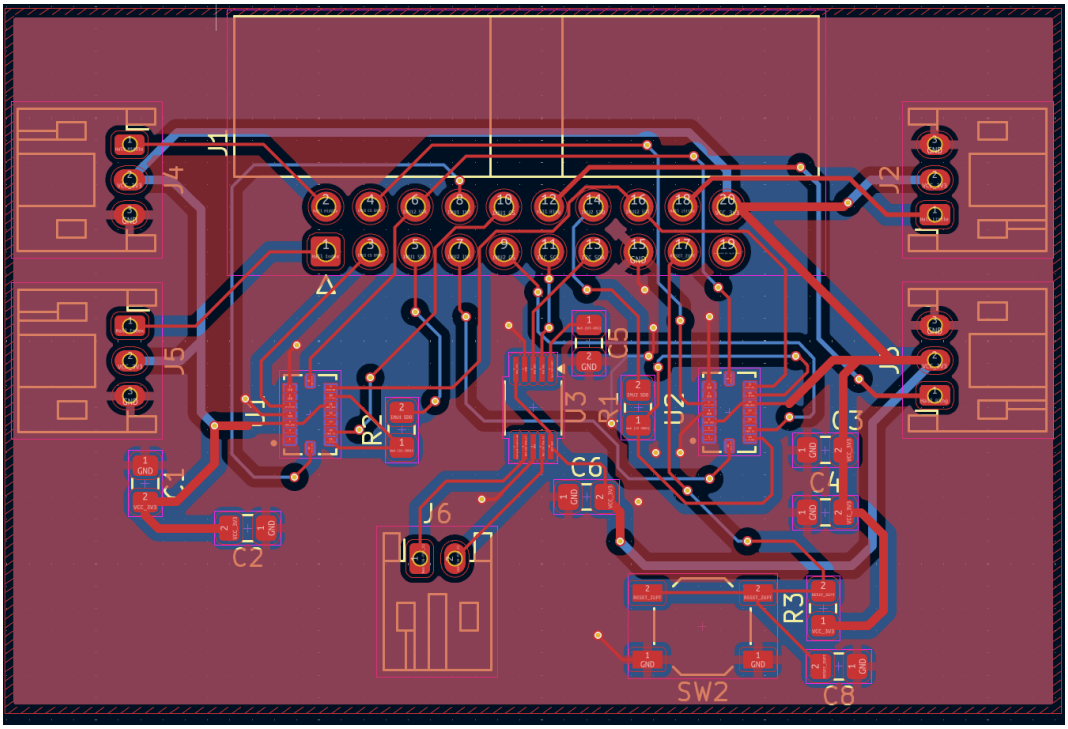

Figure 9: KiCad layout of the secondary PCB with BMI088 and DRV2605L circuitry.

Appendix B Requirements and Verification Tables

B.1 Hand Motion Tracking Subsystem RV Table

Requirement	**Verification**	**Result**
IMU must provide gravitational acceleration estimate within $\pm 5^\circ$ of actual vertical.	Collect 500-sample calibration window, compute mean vector, compare to reference gravity vector using controlled orientation jig.	Measured gravity error was $< 2.1^\circ$ across all trials.
Motion tracking must update at **100 Hz**.	Log ESP32-S3 sample timestamps and compute update frequency.	Measured 980–1000 Hz raw sampling, 100 Hz processed HID update rate.
Filtered linear acceleration must remain within deadzone when hand is stationary (no cursor drift).	Hold glove still for 10 seconds, measure cursor displacement on host PC.	Net cursor displacement remained within 3.
IMU SPI communication must show zero dropped or corrupted frames during 60-second stress test.	Enable IMU status-register polling and CRC validation while shaking glove.	0 corrupted frames observed across all tests.

Table 4: Hand Motion Tracking Subsystem Requirements and Verification

B.2 Software Subsystem RV Table

Requirement	Verification	Result
System must send cursor updates or haptic acknowledgment within **100 ms** of motion/gesture.	Use timestamped BLE debug logs + oscilloscope on haptic motor line.	Measured worst-case latency: 42 ms.
Cursor mapping must remain stable after a reset without drift.	Reset orientation, hold hand still 20 sec, track cursor drift.	Cursor drift less than 2 px over 20 seconds.
Software must correctly construct stable orthonormal control frame.	Verify orthogonality using dot-product checks on device.	$\mathbf{e_{Right}} \cdot \mathbf{e_{Up}} < 0.005$ (ideal = 0).
BLE HID packets must be sent at 80 Hz.	Record packet timing on host PC.	Measured HID rate: Significantly higher than 80 Hz.

Table 5: Software Subsystem Requirements and Verification

B.3 Finger Gesture Detection RV Table

Requirement	Verification	Result
Click detection accuracy 97% with false trigger rate less than 2%.	Run 200 cycles per finger, manually label ground truth.	Click accuracy: 98.5%; false triggers: 1.2%.
Scroll gestures must register continuously when thumb held near the ring/little finger sensor.	Hold magnet over sensor for 3 seconds, count scroll events.	Consistent level-triggered outputs; no dropout.
Hall sensors must activate when thumb is within 1 cm.	Move magnet toward sensor using caliper.	Reliable activation at 7–10 mm distance.
Hall sensor wiring must show no intermittent signals during glove movement.	Flex glove repeatedly while logging signals.	No intermittent drops observed.

Table 6: Finger Gesture Detection Subsystem Requirements and Verification

B.4 Haptic Feedback Subsystem RV Table

Requirement	**Verification**	**Result**
Haptic pulse must trigger within 50 ms of gesture confirmation.	Oscilloscope on DRV2605L output line + system timestamp logs.	Measured: 18–25 ms latency.
Haptic feedback must be perceptible but not interfere with motion sensing.	User test: perform scrolls + clicks while logging IMU noise.	Motor activation produced ¡ 2 mg disturbance (not noticeable).
DRV2605L must receive valid I²C commands 100% of time during stress-test.	Send 10,000 repeated commands while shaking glove.	All commands ACKed; 0 I²C faults.
ERM motor must operate reliably at both short (30 ms) and long (300 ms) pulses.	Trigger test waveforms repeatedly.	Motor response consistent; no startup hesitation.

Table 7: Haptic Feedback Subsystem Requirements and Verification

B.5 Power Subsystem RV Table

Requirement	Verification	Result
System must run for 2 hours under normal use.	Measure current (35 mA avg), compute battery life for 1200 mAh cell.	Estimated runtime 34 hours; requirement exceeded.
Voltage rail must remain between 3.25–3.35 V during haptic pulses.	Use oscilloscope to observe LDO output while motor runs.	Minimum observed voltage: 3.29 V.
AP2112 regulator must remain below thermal limit at 120 mA load.	Load test regulator at 130 mA for 10 minutes.	Regulator temp stabilized at 47°C (less than 85°C spec limit).
Battery protection circuitry must block overcurrent and reverse polarity.	Short output through 1 resistor; observe fuse behavior.	Polyfuse tripped instantly; system protected successfully.

Table 8: Power Subsystem Requirements and Verification